Role of ductular reaction and ductular–canalicular junctions in identifying severe primary biliary cholangitis

Authors

Diletta Overi, Guido Carpino, Laura Cristoferi, Paolo Onori, Lindsey Kennedy, Heather Francis, Nicola Zucchini, Cristina Rigamonti, Mauro Viganò, Annarosa Floreani, Daphne D'Amato, Alessio Gerussi, Rosanna Venere, Gianfranco Alpini, Shannon Glaser, Domenico Alvaro, Pietro Invernizzi, Eugenio Gaudio, Vincenzo Cardinale, Marco Carbone

Correspondence

guido.carpino@uniroma1.it (G. Carpino).

Graphical abstract

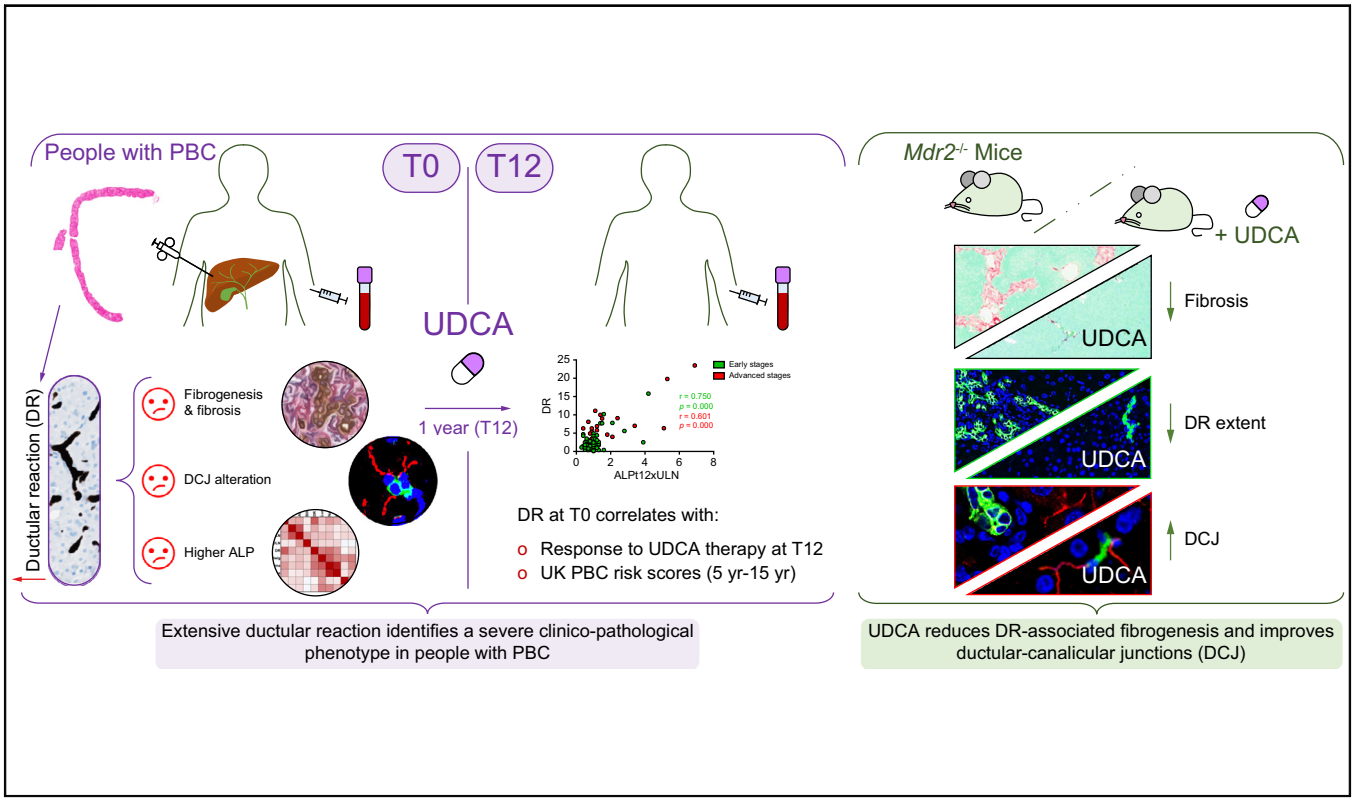

Highlights

- Ductular reaction is a histological hallmark of severe disease in people with PBC.
- Prominent ductular reaction is associated with an inadequate response to UDCA therapy.
- Ductular reaction is implied in maintaining ductular–canalicular junction integrity.
- Ductular reaction is implied in fibrogenesis in people with PBC.
- In murine cholestasis, UDCA improves ductular–canalicular junctions and fibrosis.

https://doi.org/10.1016/j.jhepr.2022.100556

Lay summary

In people affected by primary biliary cholangitis (PBC), the histological appearance of extensive ductular reaction identifies individuals at risk of progressive fibrosis. Ductular reaction at diagnosis correlates with the lack of response to first-line therapy with ursodeoxycholic acid and serves to restore ductular–canalicular junctions in people with PBC. Assessing ductular reaction extension at diagnosis may add valuable information for clinicians.

Research article

JHEP Reports

Role of ductular reaction and ductular–canalicular junctions in identifying severe primary biliary cholangitis

Diletta Overi,[1] Guido Carpino,[2,*] Laura Cristoferi,[3,4] Paolo Onori,[1] Lindsey Kennedy,[5,6] Heather Francis,[5,6] Nicola Zucchini,[3,4] Cristina Rigamonti,[7] Mauro Viganò,[8] Annarosa Floreani,[9,10] Daphne D'Amato,[3] Alessio Gerussi,[3,4] Rosanna Venere,[11] Gianfranco Alpini,[5,6] Shannon Glaser,[12] Domenico Alvaro,[11] Pietro Invernizzi,[3,4] Eugenio Gaudio,[1] Vincenzo Cardinale,[13,†] Marco Carbone[3,4,†]

[1]*Department of Anatomical, Histological, Forensic Medicine and Orthopedic Sciences, Sapienza University of Rome, Rome, Italy;* [2]*Department of Movement, Human and Health Sciences, Division of Health Sciences, University of Rome 'Foro Italico', Rome, Italy;* [3]*Division of Gastroenterology, Center for Autoimmune Liver Diseases, Department of Medicine and Surgery, University of Milano-Bicocca, Monza, Italy;* [4]*European Reference Network on Hepatological Diseases (ERN RARE-LIVER), San Gerardo Hospital, Monza, Italy;* [5]*Hepatology and Gastroenterology, Medicine, Indiana University School of Medicine, Indianapolis, IN, USA;* [6]*Richard L. Roudebush VA Medical Center, Indianapolis, IN, USA;* [7]*Department of Translational Medicine, Università degli Studi del Piemonte Orientale 'A. Avogadro', Novara, Italy;* [8]*Division of Hepatology, Ospedale San Giuseppe, University of Milan, Milan, Italy;* [9]*Studiosa Senior, University of Padua, Padua, Italy;* [10]*Scientific Consultant, IRCCS Negrar, Verona, Italy;* [11]*Department of Translational and Precision Medicine, Sapienza University of Rome, Rome, Italy;* [12]*Department of Medical Physiology, Texas A&M University College of Medicine, Bryan, TX, USA;* [13]*Department of Medico-Surgical Sciences and Biotechnologies, Sapienza University of Rome, Latina, Italy*

JHEP Reports **2022.** https://doi.org/10.1016/j.jhepr.2022.100556

Background & Aims: Primary biliary cholangitis (PBC) is a chronic cholangiopathy characterised by immuno-mediated injury of interlobular bile ducts leading to intrahepatic cholestasis and progressive liver fibrosis. PBC histology is characterised by portal inflammation, progressive fibrosis, ductopenia, and the appearance of the so-called ductular reaction. The aim of the present study was to investigate the pathogenetic relevance of ductular reaction in PBC.
Methods: Liver biopsies were collected from naïve people with PBC (N = 87). Clinical–serological parameters were obtained at diagnosis and after 1 year of ursodeoxycholic acid (UDCA) treatment. Histological staging was performed on all slides according to multiple scoring systems and criteria for PBC. Liver samples were obtained from *Mdr2*$^{-/-}$ mice treated with or without UDCA. Samples were processed for histology, immunohistochemistry, and immunofluorescence.
Results: Ductular reaction in people with PBC correlated with the disease stage and liver fibrosis, but not with disease activity; an extensive ductular reaction correlated with serum alkaline phosphatase levels at diagnosis, response to UDCA, and individuals' estimated survival, independently from other histological parameters, including disease stage. In people with PBC, reactive ductules were associated with the establishment of junctions with bile canaliculi and with fibrogenetic cell activation. Consistently, in a mouse model of intrahepatic cholestasis, UDCA treatment was effective in reducing ductular reaction and fibrosis and increasing ductular–canalicular junctions.
Conclusions: Extensive ductular reaction outlines a severe histologic phenotype in PBC and is associated with an inadequate therapy response and a worse estimated prognosis.
Lay summary: In people affected by primary biliary cholangitis (PBC), the histological appearance of extensive ductular reaction identifies individuals at risk of progressive fibrosis. Ductular reaction at diagnosis correlates with the lack of response to first-line therapy with ursodeoxycholic acid and serves to restore ductular–canalicular junctions in people with PBC. Assessing ductular reaction extension at diagnosis may add valuable information for clinicians.

Keywords: Ursodeoxycholic acid; Cholestasis; Histology; Cholangiopathy; Regeneration; Liver biopsy.
Received 17 February 2022; received in revised form 21 July 2022; accepted 3 August 2022; available online 19 August 2022
† These authors co-share the last position.
* Corresponding author. Address: Department of Movement, Human and Health Sciences, Division of Health Sciences, University of Rome 'Foro Italico', Rome, Italy. Piazza Lauro De Bosis 6, 00135-Rome, Italy. Tel./Fax: +39-06-36733-202.
E-mail address: guido.carpino@uniroma1.it (G. Carpino).

Introduction

Primary biliary cholangitis (PBC) is a chronic cholangiopathy characterised by immuno-mediated injury of interlobular bile ducts leading to cholestasis and progressive liver fibrosis.[1] PBC progression can be mitigated by therapy with ursodeoxycholic acid (UDCA), which yields numerous positive effects on the liver and biliary epithelium by improving bile flow and exerting anti-inflammatory activities.[2] Unfortunately, a relevant subgroup of people with PBC does not achieve a satisfactory biochemical

improvement after UDCA treatment, which might translate to a worse long-term outcome.[2] These people are candidates for second-line therapies, such as obeticholic acid and fibrates, which are themselves effective only in a proportion of these people, leaving an area of unmet needs.[3,4] So far, the clinical phenotypes underlying the lack of response to UDCA and a worse prognosis can be framed based on the prevailing characteristics,[5] such as ductopenia, liver failure, and portal hypertension. The leading cause(s) of the diverse disease progression have been poorly studied, and few biomarkers are available to follow people with PBC along their clinical course, whereas risk stratification at diagnosis relies only on age, histological stage, signs of hepatic dysfunction and/or portal hypertension, and liver stiffness.[6,7] Alkaline phosphatase (ALP) is a marker of cholestasis and bile duct injury and represents the pillar of the 'UDCA response'[7]; the magnitude of its reduction after UDCA therapy relates to long-term outcomes as confirmed by large-scale, observational studies.[8] However, the mechanisms underlying UDCA effects in cholestasis and the heterogeneous response in people with PBC remain to be evaluated. Therefore, the risk stratification is established after 1-year from UDCA initiation on a biochemical basis.[7]

Histologically, hallmarks of PBC are bile duct inflammation, interlobular bile duct loss, piecemeal necrosis, and liver fibrosis.[9,10] Moreover, PBC is characterised by the appearance of immature biliary epithelial cells constituting the so-called ductular reaction (DR).[11] DR cells can trigger myofibroblast activation and influence inflammatory cell recruitment, thus orchestrating a vicious circle responsible for fibrosis progression.[12,13] However, in PBC, the dynamic changes of DR phenotype and its relevance to UDCA response, disease progression, and patient prognosis is undefined.

The aims of the present study were as follows: (i) to characterise DR appearance in liver biopsies obtained from people with PBC naïve to therapy and describe its correlation with histological scoring systems and serology; (ii) to explore the correlation between DR at baseline and biochemical response after UDCA therapy; and (iii) to study the phenotypic features of DR and its association with fibrosis development and UDCA response in people with PBC and in a murine model of intrahepatic cholestasis.

Materials and methods

Extended methods are reported in the Supplementary information.

Patients

Patients were recruited from 5 sites within the Italian PBC Registry, an ongoing, noninterventional, multicentre, retrospective and prospective, observational cohort study that monitors people with PBC in Italy. All individuals with a new diagnosis of PBC and naïve to specific therapy who underwent percutaneous liver biopsy were included in this study. Diagnosis of PBC was made based on elevated ALP, the presence of antimitochondrial antibodies (AMAs) at a titre >1:40, or specific antinuclear antibodies (ANAs) immunofluorescence (nuclear dots or perinuclear rims) or ELISA results (sp100, gp210) in AMA-negative persons, or by histology.[14]

In this cohort, liver biopsy was performed to assess the disease activity and stage, as contemplated by guidelines[14] and considering the lack of non-invasive test of staging at the time of the person's first assessment.

Data on clinical, biochemical, and histological features were collected prospectively into a bespoke database. Baseline data were collected at diagnosis (*i.e.* before starting the UDCA therapy) and were as follows: age, sex, date of liver biopsy, date of diagnosis, and liver function tests performed within 3 months from the biopsy date (but before starting UDCA), that is, serum ALP, gamma-glutamyl transferase (GGT), total bilirubin (BIL), alanine aminotransferase (ALT), and aspartate aminotransferase (AST). Liver biochemistry (serum BIL, ALP, GGT, ALT, and AST) was also collected after 12 months of therapy with UDCA. The UK-PBC risk score was calculated using these laboratory investigations to estimate survival at different time frames.

As histological controls, human livers with normal histology (N = 6) were obtained from organ donors at 'Paride Stefanini' Department of General Surgery and Organ Transplantation, Sapienza University of Rome, Italy.

The study protocol conforms to the ethical guidelines of the 1975 Declaration of Helsinki as reflected in *a priori* approval by the institution's human research committee. All participants provided written informed consent. For controls, written informed consent to use tissues for research purposes was obtained from our transplant programme. No donor organs were obtained from executed prisoners or other institutionalised persons. The study was approved by the University of Milan – Bicocca Research Ethics Committee (#PBC322), coordinator of the Italian National Registry, and by the research and development department of each collaborating hospital.

Liver biopsy and histopathological evaluation

Percutaneous liver biopsies were performed according to the local standard procedure with a 16G needle in the right hepatic lobe. Only liver specimens with at least 10 complete portal tracts were considered eligible in this study. Specimens were processed for routine histology.

Histological staging was performed on all slides according to multiple histological scoring systems and criteria (Ludwig, Nakanuma, Ishak, Scheuer, and METAVIR).[6,9,10,15] For the purposes of this study, people were categorised as early (Ludwig I–II) and advanced (Ludwig III–IV) stages.

Immunohistochemistry and immunofluorescence

Sections were incubated with primary antibodies (Table S1) and processed as previously described.[11]

DR extent was quantified on cytokeratin 7 (CK7) stains using an image analysis algorithm on ImageScope (Leica Biosystems, Nussloch, Germany). Interlobular bile ducts were excluded from the counts. The presence of intermediate hepatocytes (IHs) was evaluated by staining for CK7 or epithelial cell adhesion molecule (EpCAM) in liver sections.[5]

Ductular–canalicular junctions (DCJs) were identified by immunofluorescence as the point of junction between $CK7^{pos}$ bile ductules and $ABCB11^{pos}$ canaliculi[16]; junctions were expressed as the number of junctions per portal tract or as the overall junction/ductule ratio. Proliferating cell nuclear antigen (PCNA) and Sox9 expression by DR cells was automatically calculated using an algorithm on selected DR areas and expressed as percentage of positive cells. For all other immunoreactions, the number of positive cells was automatically calculated by an algorithm, and then a semiquantitative (SQ)

score was applied (0: ≤1%; 1: 1–10%; 2: 10–30%; 3: 30–50%; 4: ≥50%).

Hepatic stellate cells (HSCs) and myofibroblasts (MFs) were evaluated by counting the number of α-smooth muscle actin (αSMA)^{pos} cells. Lobular HSCs and periportal MFs were individuated based on their location.

Murine model

Male (9–11 weeks of age) *Mdr2*$^{-/-}$ mice on FVB/NJ background were used as a model of cholestasis.[17] All mice were housed in the Indiana University Animal Facility and given free access to drinking water and standard chow. All animals received human care, and protocols strictly adhered to regulations by the Institutional Animal Care and Use Committee (IACUC) committee. Mice were fed a bile acid control (BAC) diet (N = 10) or UDCA-enriched diet (0.5% wt/wt) for 1 week (10–12 mice per group). Wild-type (WT) mice were used as controls and fed regular chow.

Histologic damage and fibrosis were assessed on routine stains. DR extent was quantified using an image analysis algorithm (ImageScope) on cytokeratin 119 (CK19)-stained slides. DCJs were individuated by immunofluorescence for CK19 and ABCB11 and counted as abovementioned. Total RNA was isolated from total liver tissues using the TRI Reagent from Sigma Life Science (Merck KGaA, Darmstadt, Germany) and reverse transcribed with the Reaction Ready First Strand cDNA Synthesis Kit (SABiosciences, Frederick, MD, USA). Selected primers were purchased from Qiagen (Valencia, CA, USA).

Statistical analysis

To account for interlaboratory variability, ALP, ALT, AST, and total BIL are expressed as a multiple of their respective upper limit of normal (ULN) values. Data are reported as mean ± SD or as median and IQR. Categorical variables are described by absolute frequencies and percentages. Student's *t* test or the Mann–Whitney *U* test was used to determine differences between groups for normally or not normally distributed data, respectively. The Pearson correlation coefficient or the Spearman nonparametric correlation was used. Multivariable linear regression model was performed. A *p* value of <0.05 was considered statistically significant. Analyses were performed using SPSS software (IBM, Milan, Italy).

Results

Patient cohort characteristics

One hundred and fifteen individuals with liver biopsy performed at diagnosis were consecutively enrolled. Among them, 19 individuals were excluded for concomitant liver diseases (12 with overlap with autoimmune hepatitis, 7 with concomitant viral hepatitis). Biopsy failure or inadequate liver specimen was recorded in 9 persons.

Eighty-seven naïve individuals with PBC with liver biopsy at diagnosis represented the study cohort. Seventy-seven (89%) were female; the median age at diagnosis was 51 years. Four persons were AMA-negative, and they were ANA gp210-positive. At baseline, median ALP, ALT, and total BIL were 1.5×ULN (IQR 1.1–2.4), 1.4×ULN (IQR 0.9–2.0), and 0.6×ULN (IQR 0.4–0.8), respectively; median liver stiffness was 6.1 (IQR/median <20%). The clinical characteristics of the cohort are reported in Table 1.

Table 1. Patient characteristics.

	Median (IQR) or n (%)
Age (years)	51.4 (49.5–64.2)
Female	n = 77 (89%)
AMA positivity	n = 83 (95.4%)
Period of diagnosis (range)	1/7/1996 to 28/5/2019
ALPt0×ULN	1.5 (1.1–2.4)
TAt0×ULN	1.4 (0.9–2.0)
TBt0×ULN	0.6 (0.4–0.8)
PLTt0×10^3/μl	234 (202–277)
ALBt0 (g/L)	42 (39–44)
ALPt12×ULN	0.96 (0.7–1.5)
TAt12×ULN	0.8 (0.5–2.1)
TBt12×ULN	0.6 (0.4–0.8)
Liver stiffness at baseline (kPa)	6.4 (4.9–8.5)

ALBt0, albumin at diagnosis; ALPt0, alkaline phosphatase at diagnosis; ALPt12, alkaline phosphatase after 12 months of treatment with UDCA; AMA, anti-mitochondrial antibody; PLTt0, platelet count at diagnosis; TAt0, transaminases at diagnosis; TAt12, transaminases after 12 months of treatment with UDCA; TBt0, total bilirubin at diagnosis; TBt12, total bilirubin after 12 months of treatment with UDCA; UDCA, ursodeoxycholic acid; ULN, upper limit of normal.

Correlation between DR and histopathologic scoring

Liver biopsies from all individuals were characterised according to histopathological scoring systems (Fig. 1 and Table S2). DR was evaluated as the extent of CK7^{pos} ductules at the interface with portal tracts, whereas IHs were recognised as cells with an intermediate phenotype between hepatocyte and biliary epithelial cells, displaying EpCAM and/or CK7 positivity and in continuous with reactive ductules (Fig. 1A).

Both DR and IH significantly correlated with histologic disease stage as defined by standardised scoring systems (Fig. 1B). When single elements of the Nakanuma staging system were separately considered, both DR and IHs significantly correlated with fibrosis (r = 0.540 and r = 0.505, respectively; p <0.001) and interlobular bile duct loss (r = 0.429 and r = 0.615, respectively; p <0.001). Accordingly, DR and IHs correlated with fibrosis stage assessed using Ludwig, Scheuer, METAVIR, and Ishak scoring systems (Fig. 1B). DR did not correlate with grading according to the Nakanuma system (*i.e.* hepatitis activity [HA] and cholangitis activity [CA]). The number of IHs slightly but significantly correlated with HA (r = 0.276, p = 0.016) but not with CA (Fig. 1B).

To further explore the relationship between DR and fibrosis, grouped analyses were performed by stratifying people into the 4 Ludwig stages and by polling the stages into early (Ludwig I–II) and advanced (Ludwig III–IV) categories. Advanced stages were characterised by significantly increased DR extent (Fig. 1C) and IH score (Table S3) compared with early stages. Similar results were obtained when people were stratified based on fibrosis stage according to METAVIR (Fig. 1D and Table S3).

Taken together, these results suggest that the extent of DR and the presence of intermediate hepatocytes correlated with PBC disease stage and fibrosis but not with disease activity. When we evaluated each histologic modification in individual Ludwig stages, our data showed that HA and CA mostly increased in early stages ('florid stages'), whereas bile duct loss and DR progressively reached their maximum values in stage IV (Fig. S1).

DR correlates with serum ALP

Next, we evaluated the correlation between liver histology and liver biochemistry at baseline (ALPt0, ALTt0, ASTt0, and BILt0; Fig. 2A). DR resulted strongly correlated with ALPt0 (r = 0.644, p <0.001), and slightly but significantly with ALTt0 (r = 0.326, p = 0.002) and BILt0 (r = 0.241, p = 0.026). In comparison, PBC stages

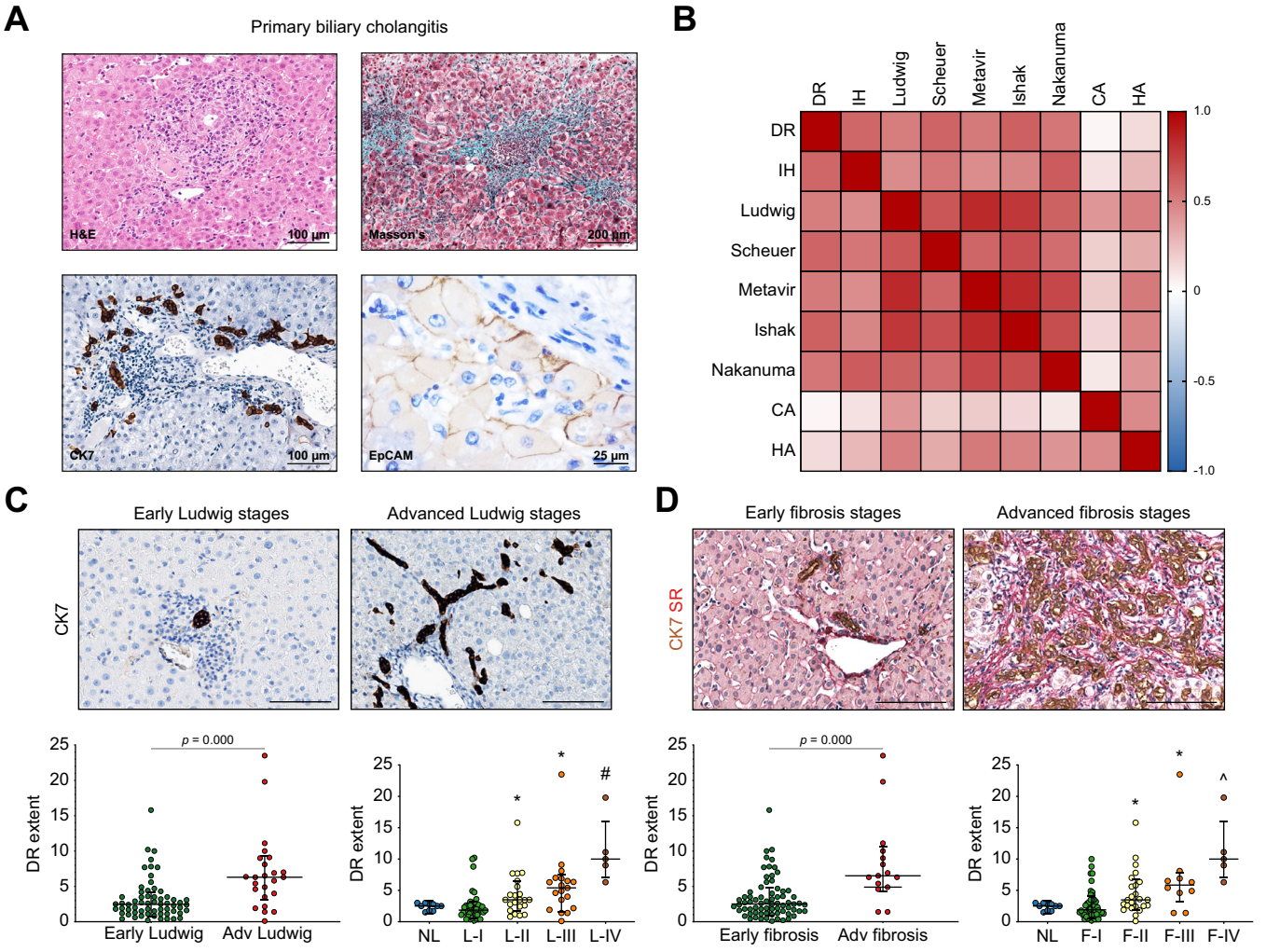

Fig. 1. DR and histology in PBC. (A) H&E, Masson's trichrome, and immunohistochemistry for CK7 and EpCAM (for IHs) in PBC liver biopsies. (B) Pearson correlation coefficients. (C) CK7 in early (I/II) and advanced (III/IV) Ludwig stages. (D) CK7-stained slides were counterstained with SR to visualise the relationship between DR and fibrosis. C and D: scale bars = 100 μm. Plots show medians (IQR) for DR according to Ludwig (L) and METAVIR (F). *p <0.05 *vs.* L–I or F–I and NL; #p <0.05 *vs.* all; ^p <0.05 *vs.* F–I/F–II/NL (Mann–Whitney *U* test). CA, cholangitis activity; CK7, cytokeratin 7; DR, ductular reaction; EpCAM, epithelial cell adhesion molecule; HA, hepatitis activity; IH, intermediate hepatocyte; NL, normal liver; PBC, primary biliary cholangitis; SR, Sirius red.

by Nakanuma and Ludwig were only slightly correlated with ALPt0 (r = 0.395, p <0.001, and r = 0.248, p = 0.021, respectively) and ASTt0 (r = 0.247, p = 0.049 and r = 0.250, p = 0.046, respectively). No correlation was found between histologic grading and serum biochemistry. Of note, multivariate linear regression analysis demonstrated DR to be significantly correlated with ALPt0 (beta = 0.684, p = 0.001), independently of the other histological parameters included in the analysis (*i.e.* IH score and Ludwig, Scheuer, METAVIR, Ishak, and Nakanuma histological scores).

A heat map based on hierarchic clustering of people divided according to ALP levels (grouped into ALPt0^{low} if ALPt0×ULN <1.5 and ALPt0^{high} if ALPt0×ULN ≥1.5) confirmed the close relationship between ALP with DR and IH, particularly in people with advanced stage (Fig. 2B). DR extent significantly increased in people with PBC with elevated ALP serum levels (ALPt0^{high}: 5.8 ± 5.0%) but not in those with relatively low ALP serum levels (ALPt0^{low}: 2.7 ± 2.2%) compared with controls (2.4 ± 0.5%; p <0.05; Fig. 2C). Accordingly, ALPt0 levels were higher in people with PBC with biopsies containing clusters of intermediate hepatocytes (Fig. 2D).

DR predicts response to UDCA therapy and survival

We then explored whether the extent of DR at baseline could relate to the response to UDCA therapy. We first assessed the correlation between DR extension and other histological parameters with the estimated UDCA response by the UDCA response score (URS) and with the observed response (defined by ALP at 12 months after UDCA therapy [ALPt12]) in our entire cohort.

DR was found to be strongly and inversely correlated with URS (r = −0.738, p <0.001) and strongly and positively correlated with ALPt12 (r = 0.734, p <0.001). The correlation matrix (Fig. 3A) shows that ALPt12 was correlated with histologic staging and fibrosis but not with disease grading. Of note, DR was the histopathological variable with the strongest correlation value. Moreover, at multivariate linear regression analysis, DR was a significant predictor of ALPt12 (beta = 0.734, p <0.001),

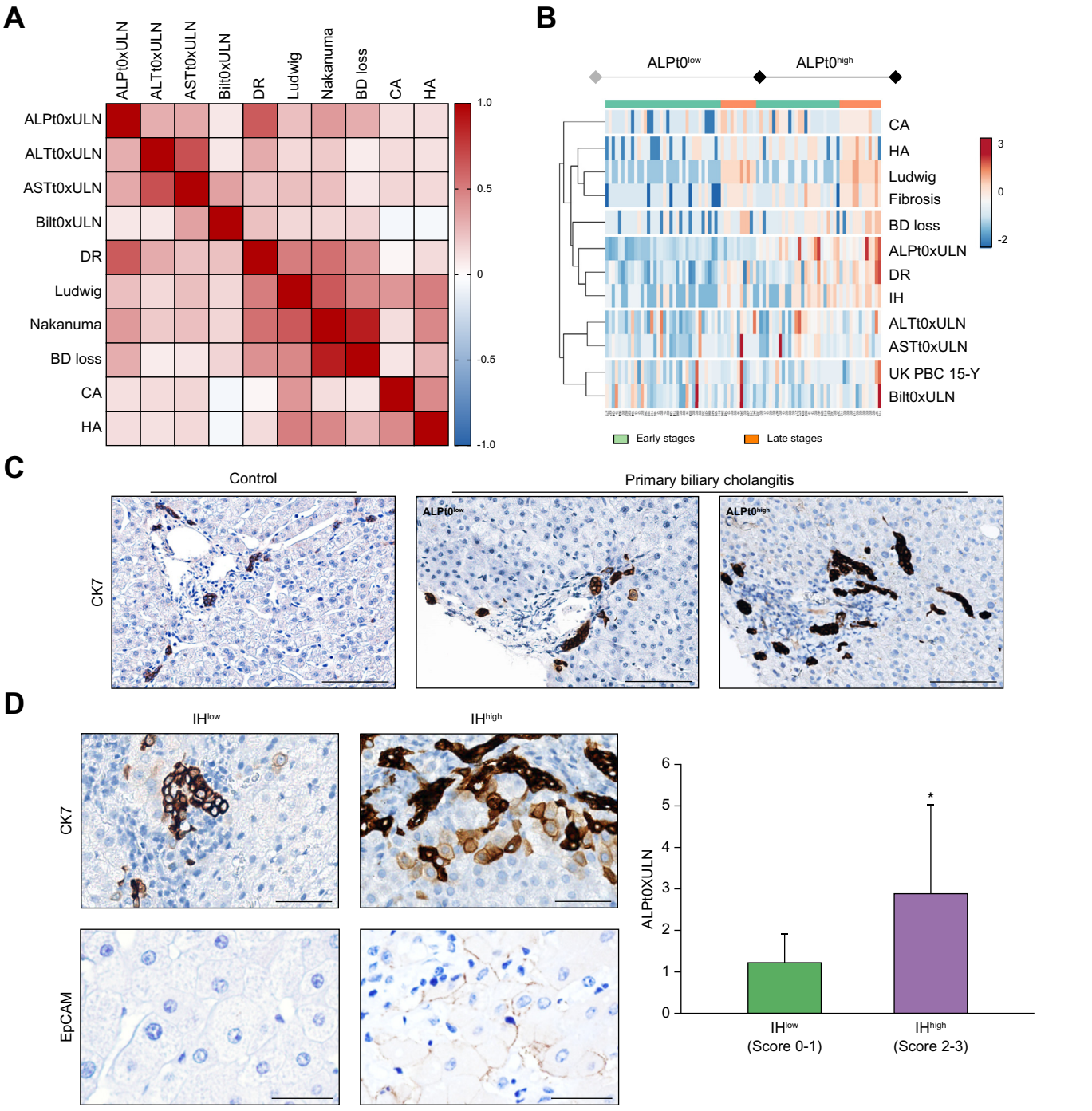

Fig. 2. DR and clinical parameters at baseline in PBC. (A) Pearson correlation coefficients. (B) Hierarchical clustering of people divided according to ALPt0×ULN <1.5 (ALPt0^{low}) or ALPt0×ULN ≥1.5 (ALPt0^{high}). (C) CK7 in controls and people with PBC. Scale bar: 100 μm. (D) CK7 and EpCAM in people with PBC. People with higher IHs showed higher ALPt0×ULN values. Scale bars: 25 μm. Histogram shows means (SD) for ALPt0×ULN. *p <0.05 (Mann–Whitney U test). ALPt0, alkaline phosphatase at diagnosis; ALTt0, alanine aminotransferase at diagnosis; ASTt0, aspartate aminotransferase at diagnosis; BD, bile duct; Bilt0, bilirubin at diagnosis; CA, cholangitis activity; CK7, cytokeratin 7; DR, ductular reaction; EpCAM, epithelial cell adhesion molecule; HA, hepatitis activity. IH, intermediate hepatocyte; PBC, primary biliary cholangitis; ULN, upper limit of normal.

independently of the other histological parameters included in the analysis (*i.e.* IH score and Ludwig, Scheuer, METAVIR, Ishak, and Nakanuma scores).

We then evaluated whether DR could add prognostic value in stratifying people with PBC within the same histologic stage (*i.e.* Ludwig stage; Fig. 3B), and we observed that DR correlated with ALPt12 in people at both early and advanced Ludwig stages (r = 0.750, p <0.001, and r = 0.601 p <0.001, respectively). Correlations in individual Ludwig stages are reported in Table S4 and Fig. S2.

Then, people were divided according to ALP levels at baseline (Fig. 3C and Fig. S3). In people with ALPt0×ULN <1.5, DR did not correlate with ALPt12 and URS, whereas DR strongly correlated

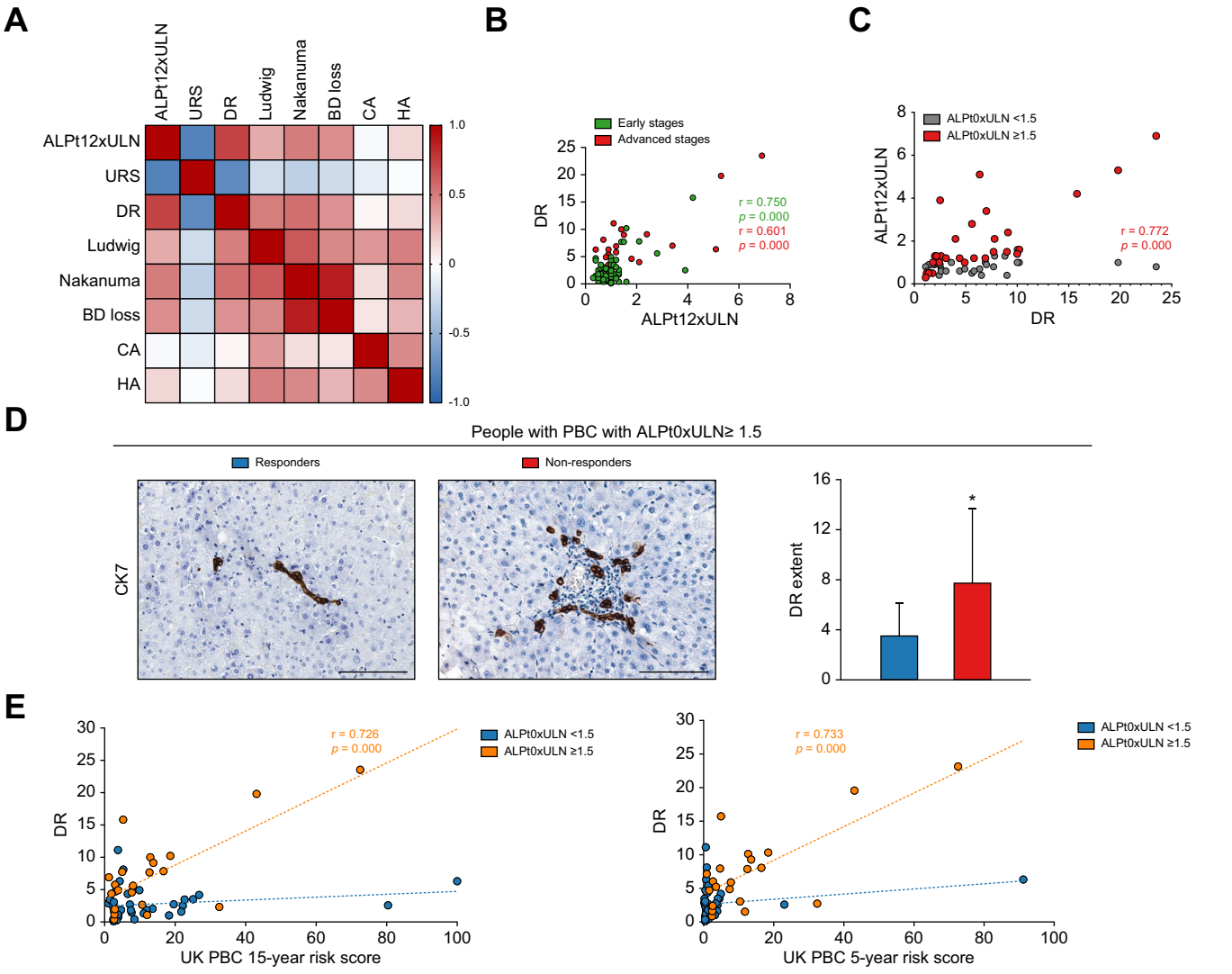

Fig. 3. DR and clinical parameters after UDCA treatment in PBC. (A) Heat map reports Pearson correlation coefficients. (B and C) Pearson correlation coefficients for DR and ALPt12×ULN. Early/advanced Ludwig stages (B) and people with ALPt0×ULN <1.5 or ALPt0×ULN ≥1.5 (C) are in different colours. (D) CK7 in people with PBC with ALPt0×ULN ≥1.5. Scale bars: 100 μm. Histogram shows means (SD) for DR. *p <0.05 (Student's t test). (E) Pearson correlation coefficients between DR and UK-PBC risk scores subdividing people according to ALPt0×ULN. ALP, alkaline phosphatase; ALPt0, ALP at diagnosis; ALPt12, ALP after 12 months of UDCA; BD, bile duct; CA, cholangitis activity; CK7, cytokeratin 7; DR, ductular reaction; HA, hepatitis activity; PBC, primary biliary cholangitis; ULN, upper limit of normal; UDCA, ursodeoxycholic acid; URS: UDCA response score.

with ALPt12 and URS in people with ALPt0×ULN ≥1.5 (r = 0.772 and r = −0.749, respectively; p <0.001).

Finally, people with ALPt0×ULN ≥1.5 were studied separately and further subdivided, according to the reduction of ALP below the therapeutic target of 1.5 at 12 months after UDCA therapy, into responders and non-responders (*i.e.* UDCA responders according to Paris II criteria; Fig. 3D). DR at baseline was significantly lower in UDCA responders (3.5 ± 2.6%) than in UDCA non-responders (8.9 ± 6.3%; p = 0.002). Of note, people in these two subgroups did not differ in terms of disease stage. These results define a correlation between DR and the liver biochemistry after UDCA therapy, particularly in people in a more advanced stage and with a more active disease at baseline.

To study the prognostic role of DR on the estimated survival, its extent was correlated with the *UK-PBC risk scores* (Fig. 3E). In the entire cohort, DR extent significantly correlated with UK-PBC risk scores at 15 and 10 years (r = 0.381, p = 0.002, and r = 0.319, p = 0.012, respectively) but not with the 5-year risk scores (r = 0.184, p = 0.155). Interestingly, when the analysis was restricted to people with elevated ALPt0 (ALPt0^{high}), the correlations between DR and UK-PBC scores were increased (15-year risk score: r = 0.726, p <0.001; 10-year risk score: r = 0.732, p <0.001; 5-year risk score: r = 0.733, p <0.001).

These results suggest that DR correlates with the liver function tests, particularly with ALP, and holds prognostic meaning toward long-term outcomes.

Phenotype of DR and DCJs in people with PBC

Next, we hypothesised that, given its choleretic effects, the effective response to UDCA administration could be related to the presence of a functional bile drainage, assured by the anatomical continuity between the hepatocyte canalicular

system and the interlobular bile ducts via the bile ductules and DCJ. Therefore, we aimed to determine whether DR response was directed to the replacement of immune-damaged interlobular bile ducts and/or the reconstitution of the DCJs. Thus, we evaluated a subgroup of 30 individuals, representative of the entire cohort (90% women, median age 52 years) and included a series of non-diseased liver samples as controls. On these specimens, we evaluated the following: (i) the expression of the progenitor cell marker Sox9; (ii) the phenotype of DR in terms of mature cholangiocyte commitment/differentiation (*i.e.* secretin receptor [SCTR] and mucin 1 [Muc-1]); and (iii) the number of DCJs by immunofluorescence for CK7 and ABCB11.

DR in PBC samples displayed high Sox9 expression (48.6 ± 26.5%) with no differences compared with control livers (54.4 ± 23.1%; Fig. 4A). Sox9 expression in people with PBC was correlated with the extent of DR (r = 0.702, p <0.01). Reactive ductules expressed variable levels of mature cholangiocyte markers (SQ score for SCTR: 1.6 ± 1.3 and that for Muc-1: 0.4 ± 0.7), which were reduced compared with normal livers (SQ score for SCTR: 3.3 ± 0.8 and that for Muc-1: 1.7 ± 0.5; p <0.008 and p <0.004, respectively; Fig. 4B). No correlations were found between the expression of mature cholangiocyte markers and DR extent or other studied variables.

The study of established junctions between hepatocyte canaliculi and the reactive ductules (DCJs) revealed a significantly lower number of the DCJs per portal tract ($DCJ^{/pt}$) and per ductule ($DCJ^{/d}$) in people with PBC ($DCJ^{/pt}$: 0.72 ± 0.67; $DCJ^{/d}$: 0.27 ± 0.25) than in controls ($DCJ^{/pt}$: 1.67 ± 0.41; $DCJ^{/d}$: 0.57 ± 0.08; p = 0.002 and p = 0.006, respectively; Fig. 4C and D and Fig. S4). The DCJ number was not influenced by PBC histological stage, as indicated by the lack of significant differences between early and advanced Ludwig stages. Of note, DCJs were associated with the entity of biochemical cholestasis as demonstrated by their lower number in individuals with ALPt0×ULN ≥1.5 than in those with ALPt0×ULN <1.5 (Fig. 4E and Fig. S4). Finally, DCJ numbers in PBC biopsies were significantly correlated with DR extent ($DCJ^{/pt}$: r = 0.452, p = 0.018; $DCJ^{/d}$: r = 0.486, p =0.010).

These results suggest that, in patients, DR lacks differentiation towards mature cholangiocyte functions, but it is aimed, at least partially, at re-establishing DCJ; however, in people with severe cholestasis, DR might fail to develop DCJ.

DR correlates with the fibrogenetic cell pool

Because DR is considered a main driver of liver fibrogenesis in several human diseases, we next evaluated its possible correlation with the liver fibrogenetic cell pool (*i.e.* lobular HSCs and periportal MFs) in our sub-cohort of 30 individuals (Fig. 5). PBC biopsies were characterised by a higher number of lobular and periportal HSCs (4.9 ± 2.7 and 6.39 ± 4.9, respectively) with control livers (2.8 ± 1.1, p = 0.044; 2.7 ± 0.5, p = 0.048, respectively). Lobular and periportal HSCs were significantly higher in advanced (6.2 ± 2.8, p = 0.008, and 10.6 ± 6.4, p = 0.004, respectively) but not in early PBC stages (4.3 ± 2.6 and 4.4 ± 2.3, respectively; p >0.05) with controls; moreover, periportal HSCs but not lobular HSCs were significantly increased in advanced PBC compared with early PBC stages (p = 0.005). Remarkably, the number of lobular and periportal HSCs significantly correlated with DR extent (r = 0.761, p <0.001, and r = 0.878, p <0.001, respectively), Nakanuma fibrosis score (r = 0.514, p = 0.024, and r = 0.487, p = 0.035, respectively), ALPt0 (r = 0.607, p = 0.006, and r = 0.866, p <0.001, respectively), and ALPt12 (r = 0.820, p <0.001, and r = 0.792, p <0.001, respectively).

DR response to UDCA: *in vivo* model

Finally, a mouse model of intrahepatic cholestasis and DR-associated fibrosis ($Mdr2^{-/-}$ mice) was used to test the potential effect of UDCA on DR and its association with portal fibrosis. As expected, the livers explanted from $Mdr2^{-/-}$ + BAC mice were characterised by hepatocyte necrosis, fibrosis, and a prominent DR compared with control mice (Fig. 6). When fed UDCA diet, $Mdr2^{-/-}$ mice showed a significantly lower fibrosis, αSMA^{pos} cell number, and DR extent than $Mdr2^{-/-}$ + BAC mice (Fig. 6 and Table S4). No difference in hepatocyte necrosis was present between $Mdr2^{-/-}$ + BAC and $Mdr2^{-/-}$ + UDCA mice. Interestingly, portal fibrosis was spatially associated with reactive ductules, and its extent correlated with DR within the same portal tract (r = 0.76, p = 0.0097; Fig. 6).

DR in $Mdr2^{-/-}$ + BAC mice was characterised by a higher percentage of $Sox9^{pos}$ cells with WT mice (Fig. 7A). $Mdr2^{-/-}$ mice fed UDCA diet showed a significant reduction in $Sox9^{pos}$ DR cells compared with $Mdr2^{-/-}$ + BAC mice (Fig. 7A and Table S5). When markers of mature cholangiocytes were studied, $Mdr2^{-/-}$ + BAC mice showed a significant reduction of anion exchanger 2 (AE2) and SCTR expression compared with WT by both immunofluorescence and real-time quantitative PCR (RT-qPCR) analyses (Fig. 7B and C); moreover, $Mdr2^{-/-}$ + BAC mice showed a marked reduction in DCJ number both per bile duct and per portal tract compared with WT mice (Fig. 7C). UDCA administration did not induce a significant upregulation of mature cholangiocyte gene expression (Fig. 7B and C), but it determined the increase in the number of connections between bile ductules and hepatocyte bile canaliculi as demonstrated by immunofluorescence (Fig. 7D).

Discussion

The present study demonstrates the following: (i) DR extent in people with PBC is correlated with the disease stage and progressive liver fibrosis, but not with inflammatory disease activity; (ii) DR extent is correlated with serum ALP levels; (iii) an extensive DR is correlated with reduced chances to respond to UDCA treatment and with patients' prognosis; (iv) DR is associated with the establishment of junctions with bile canaliculi and with fibrogenetic pool activation; and (v) in a mouse model of intrahepatic cholestasis, UDCA treatment is effective in reducing DR and fibrosis and increasing DCJs. As a follow-up of our previous work to determine the nature of UDCA treatment failure and to develop a predictive model of response that would enable accurate identification of people unlikely to respond to UDCA,[5] the findings of the present study shed new light in the understanding of the mechanisms underlining the response to UDCA and the effects of the drug.

DR is a histologic hallmark of parenchymal and biliary chronic damage.[13,18] Although DR is generally prominent in people with PBC, the clinical implications of its appearance and its significance in disease pathogenesis have not been fully characterised. Previously, we described the phenotype of DR in explant livers of people with PBC.[11,19] In the present study, we evaluated DR phenotype in a relatively large cohort of biopsy-proven, naïve people with PBC undergoing UDCA treatment. Liver biopsies were obtained from both AMA-negative and AMA-positive individuals with PBC and from people with mild disease. This can be, at least in part, explained by the historical experience in viral hepatitis in Italy, which might have made liver physicians more prone to stage chronic disease by liver biopsy.

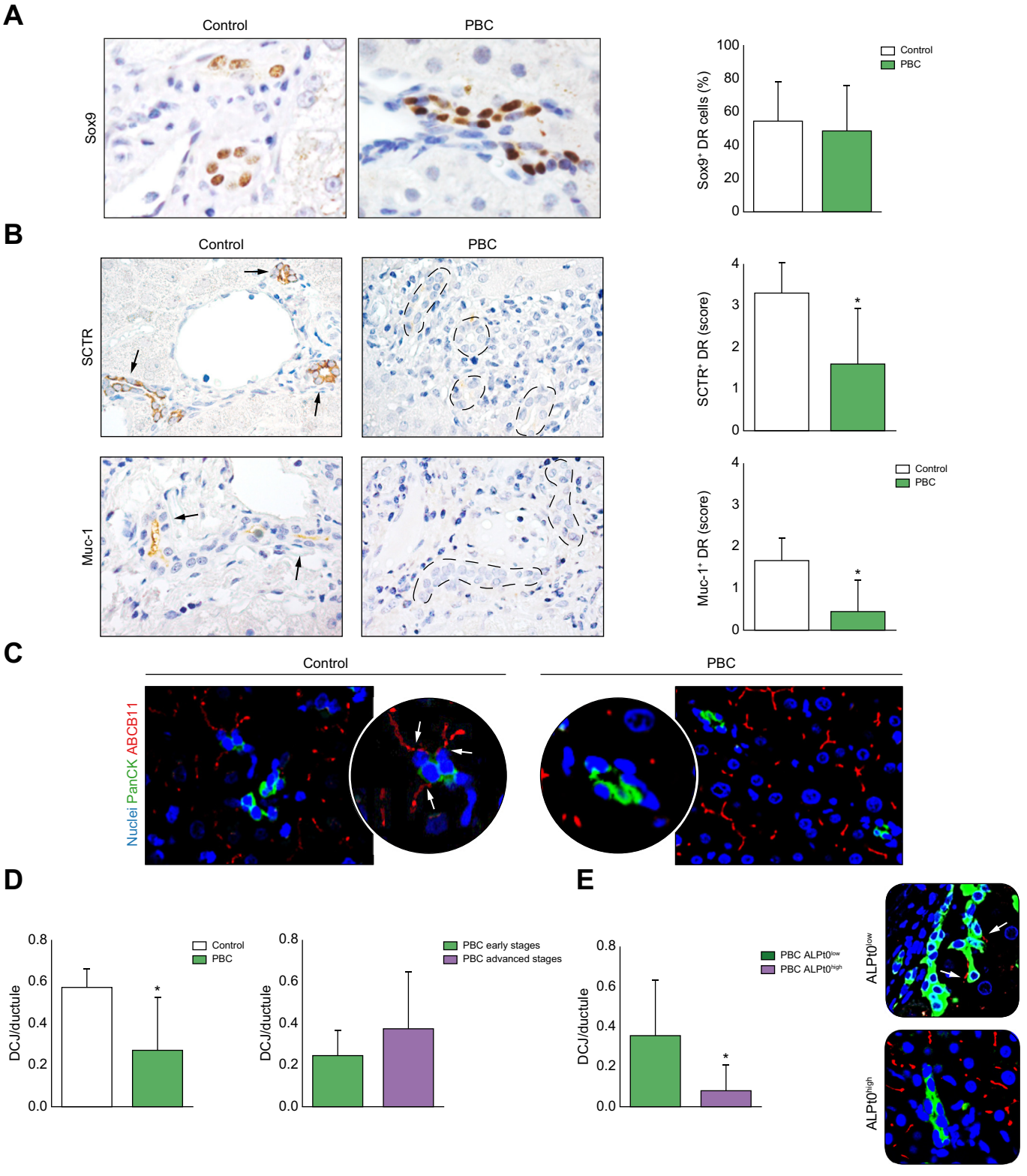

Fig. 4. DR phenotype in PBC. (A) Immunohistochemistry for Sox9 in controls and PBC. Magnification: 40×. (B) SCTR and Muc-1 in controls and PBC. Arrows: positive cells. Dotted lines: negative ductules. Histograms (A/B) show means (SD) for positive cells. $^{*}p$ <0.001 (Mann–Whitney *U* test). (C) Double immunofluorescence for PanCK/ABCB11. Arrows: DCJ. (D) Histograms show means (SD) for DCJ/ductule in controls *vs.* PBC, and PBC at early *vs.* advanced Ludwig stages. $^{*}p$ <0.01 (Mann–Whitney *U* test). (E) Means (SD) for DCJ/ductule in people with ALPt0×ULN <1.5 ($ALPt0^{low}$) or ALPt0×ULN ≥1.5 ($ALPt0^{high}$). $^{*}p$ <0.05 (Mann–Whitney *U* test). Double IF for PanCK/ABCB11 in PBC. Arrows: DCJ. Magnification (A–B/D): 20×. ALPt0, ALP at diagnosis; DCJ, ductular–canalicular junction; DR, ductular reaction; Muc-1, mucin 1; PBC, primary biliary cholangitis; SCTR, secretin receptor; ULN, upper limit of normal.

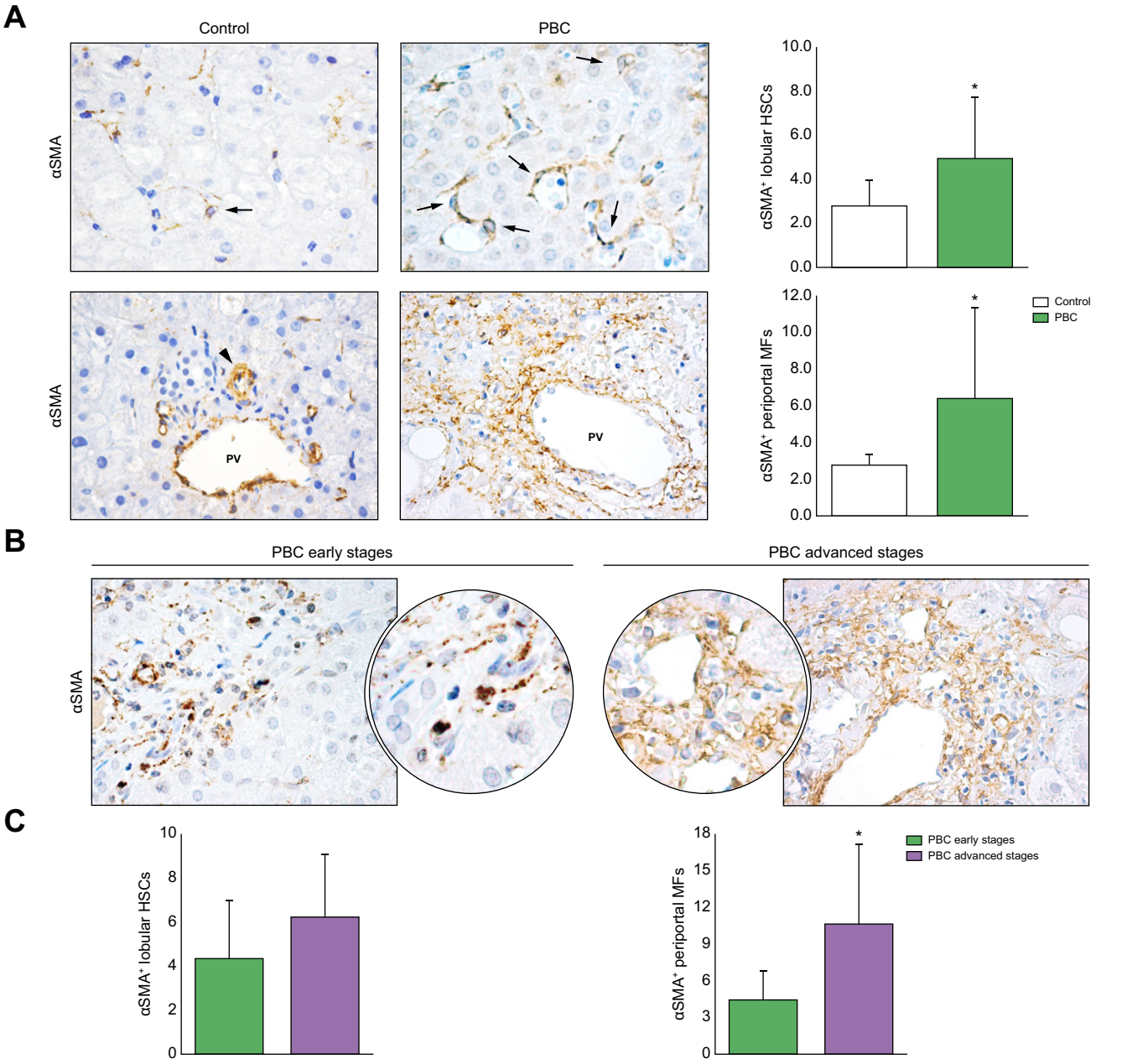

Fig. 5. Activation of fibrogenetic pool in PBC. (A) Immunohistochemistry for αSMA in controls and people with PBC individuates HSCs (upper panels, arrows) and portal MFs (lower panels). Arrowhead: αSMA^{pos} artery within portal tract. Magnification: 40×. Histograms show means (SD) for αSMA^{pos} cells. $^{*}p$ <0.05 (Mann–Whitney *U* test). (B) Immunohistochemistry for αSMA in early (I/II) and advanced (III/IV) Ludwig stages of PBC. Areas in the circles are magnified. Magnification: 40×. (C) Histograms show means (SD) for αSMA^{pos} cells according to the Ludwig stage. $^{*}p$ <0.05 *vs.* early Ludwig stages (Mann–Whitney *U* test). αSMA, α-smooth muscle actin; HSC, hepatic stellate cell; MF, myofibroblast; PBC, primary biliary cholangitis; PV, portal vein.

Here, we described a significant correlation between DR extent and disease stage, but not with disease activity. This aspect could explain the dynamic of the disease course in PBC: early stages are characterised by florid, portal inflammation and interface hepatitis; as disease progresses, the development of significant biliary fibrosis occurs, prompted by DR expansion.[1,10,20]

We found a significant correlation between DR and ALP levels at baseline, independent of other histological parameters. This is remarkable because ALP elevation represents the hallmark of chronic cholestasis and biliary injury in PBC and is currently used as a reference to assess treatment response.[8] Accordingly, DR extent correlated also with patient response to UDCA and long-term prognosis estimated by the UK-PBC score.

UDCA treatment response represents a cornerstone of risk stratification in PBC as it enables to discriminate the long-term outcome of patients.[21] We hypothesised that the magnitude of UDCA response was secondary to the extent of the underlying biliary damage. Herein, we described a correlation between DR extent at the index biopsy and ALP levels after 1 year of UDCA treatment. The correlation between both ALPt0 and ALPt12 and DR appeared to be independent from other histological parameters including fibrosis stage. This is particularly relevant given

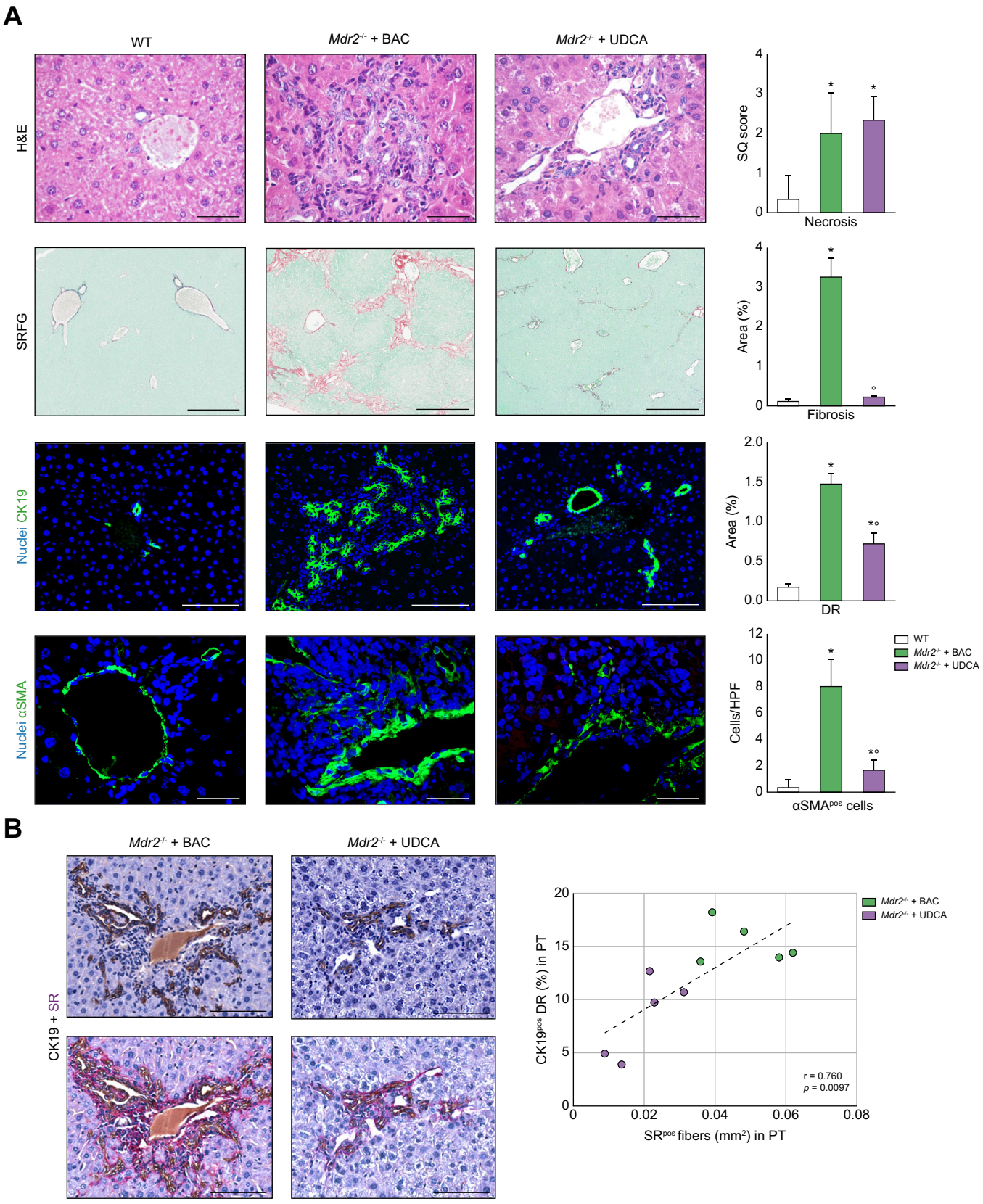

Fig. 6. Liver injury, hepatic fibrosis, and ductular reaction after UDCA administration in *Mdr2*$^{-/-}$ mice. (A) H&E, SRFG, and immunofluorescence for CK19 and αSMA in controls (WT) and *Mdr2*$^{-/-}$ mice fed BAC (*Mdr2*$^{-/-}$ + BAC) or UDCA-enriched (*Mdr2*$^{-/-}$ + UDCA) diets. Scale bars: 100 μm (H&E/CK19), 150 μm (SRFG), and 50 μm (αSMA). Histograms: means (SD) for hepatocyte necrosis, fibrosis, DR, and αSMA^{pos} cells. *p <0.05 *vs.* WT; ◦p <0.05 *vs.* *Mdr2*$^{-/-}$ + BAC (Mann–Whitney *U* test). (B) CK19-stained sections counterstained with SR show the relationship between DR and fibrosis. Scale bars: 100 μm. Scatterplot shows Pearson correlation coefficients between DR and SR^{pos} fibres around PTs. αSMA, α-smooth muscle actin; BAC, bile acid control; CK19, cytokeratin 19; DR, ductular reaction; HPF, high-powered field; PT, Sirius red/fast green; SQ, semiquantitative; SR, Sirius red; SRFG, Sirius red/fast green; UDCA, ursodeoxycholic acid; WT, wild type.

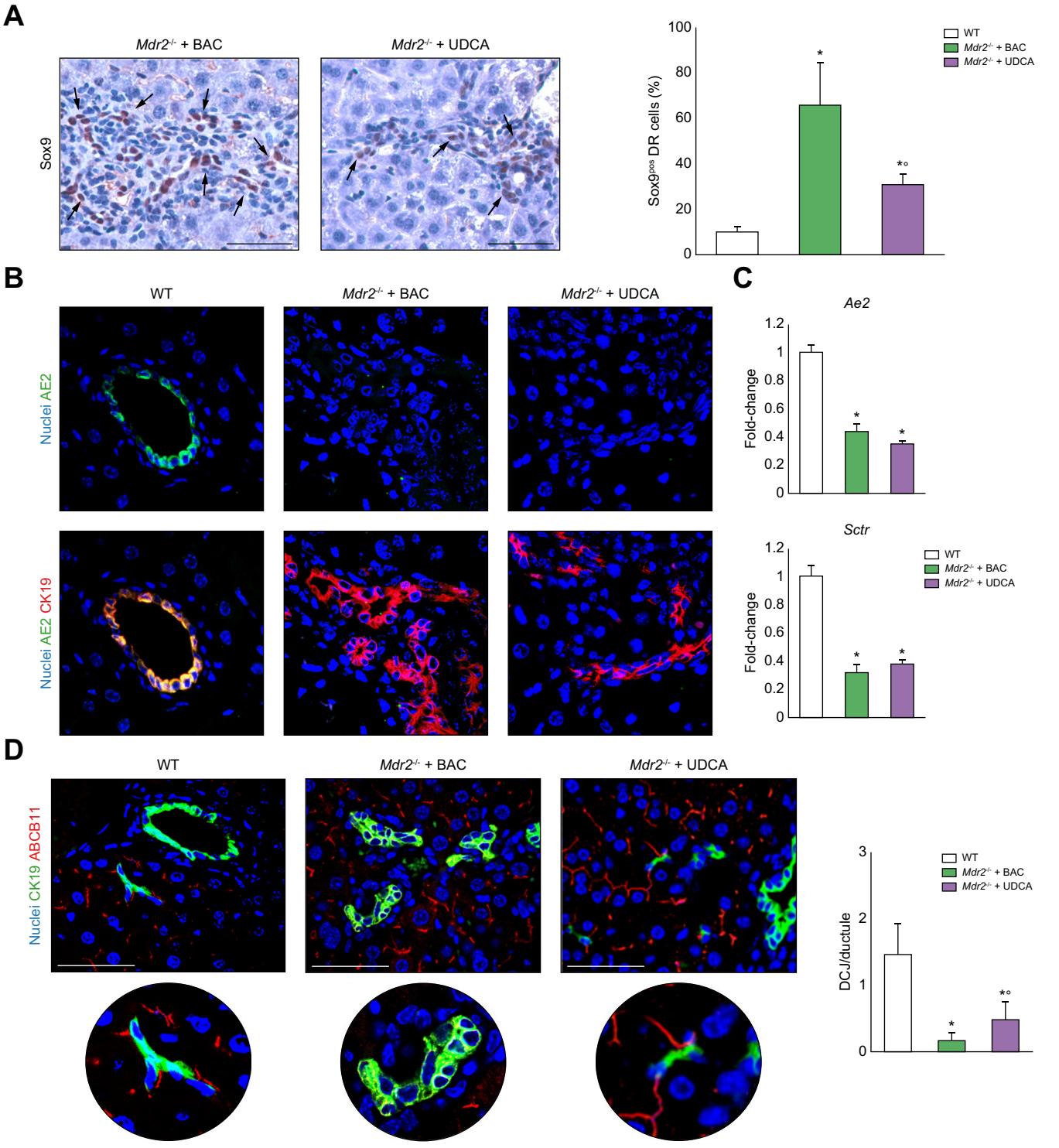

Fig. 7. DR phenotype after UDCA administration in *Mdr2*$^{-/-}$ mice. (A) Immunohistochemistry for Sox9 in *Mdr2*$^{-/-}$ mice fed BAC (*Mdr2*$^{-/-}$ + BAC) or UDCA-enriched (*Mdr2*$^{-/-}$ + UDCA) diets. Arrows: Sox9^{pos} cells. Scale bars: 50 μm. Histogram shows means (SD) for Sox9^{pos} DR cells. (B) Immunofluorescence for AE2 and CK19 in controls (WT) and *Mdr2*$^{-/-}$ + BAC and *Mdr2*$^{-/-}$ + UDCA mice. Separate channels are provided. (C) Histograms show means (SD) for RT-qPCR of *Ae2* and *Sctr* in mice liver. (D) Immunofluorescence for CK19 and ABCB11. Scale bars: 50 μm. Histogram shows means (SD) for DCJ/ductule. *p <0.05 *vs.* all. *p <0.05 *vs.* WT; ◦p <0.05 *vs.* *Mdr2*$^{-/-}$+BAC (Mann–Whitney *U* test). AE2, anion exchanger 2; BAC, bile acid control; CK19, cytokeratin 19; DCJ, ductular–canalicular junction; DR, ductular reaction; RT-qPCR, real-time quantitative PCR; UDCA, ursodeoxycholic acid; WT, wild type.

the association between fibrosis progression and poor prognosis in people with PBC.[20,22–24] Indeed, advanced histologic fibrosis at baseline is reported as an independent predictor of survival beyond biochemical treatment response at 1 year.[25] Given the increase of ALP levels in other biliary and liver conditions (*e.g.* primary sclerosing cholangitis and non-alcoholic fatty liver disease), future studies addressing the correlation between ALP and DR in other diseases may further clarify whether or not this relationship is a unique feature of PBC pathogenesis.

Next, we elucidated the potential regenerative pathways at the basis of DR onset in people with PBC. Previous studies demonstrated that DR appearance is constituted of hepatic progenitor cells activated in supporting hepatocyte or cholangiocyte regeneration.[11,19,26] Because interlobular bile ducts are the target of autoimmune injury in PBC, we hypothesised that DR would be activated in supporting biliary tree regeneration, as suggested by the correlation between DR and bile duct loss observed in our cohort. Therefore, we assessed DR phenotype; surprisingly, reactive ductules showed low or negligible levels of mature cholangiocyte marker expression (*i.e.* SCTR and Muc-1) and maintained a predominantly immature phenotype (Sox9 expression). In normal conditions, bile ductules are the point of connection (DCJ) between the hepatocyte bile canaliculi and the bile duct system; the integrity of this connection has a pivotal role in physiologic bile flow.[16] In our cohort, we observed a progressive destruction of DCJs in people with PBC, associated with ALP elevation. Remarkably, DR extent correlated with the number of DCJs, suggesting a role for reactive ductules in restoring the anatomical connection with bile canaliculi as a compensatory mechanism for favouring bile flow.

In addition to the beneficial effect on DCJ integrity, DR extent correlated with the activation of fibrogenetic cells; this explains the correlation between DR and progressive fibrosis in our cohort and supports the concept of a fibrogenetic niche surrounding proliferating ductules as observed in other liver diseases.[13,27]

To support our observation in patients, we studied an experimental model of intrahepatic cholestasis, the *Mdr2*$^{-/-}$ mouse.[17] Although *Mdr2*$^{-/-}$ mice do not fully recapitulate PBC pathogenesis, these animals develop extensive DR-associated biliary fibrosis as a consequence of altered bile composition, caused by impaired phospholipid secretion at the hepatocyte canalicular level.[28,29] Moreover, given the lack of models mimicking all PBC histologic features, the *Mdr2*$^{-/-}$ model was used to understand the dynamics of DR, biliary fibrosis, DCJ, and response to UDCA in intrahepatic cholestasis. In these mice, the number of DCJs was significantly reduced, and DR was triggered. Remarkably, UDCA treatment led to an increase of the DCJ number, together with a significant reduction of DR extent and fibrosis.

In conclusion, extensive DR is a histological feature of PBC that outlines a severe histologic phenotype characterised by bile duct inflammation, ductopenia, and progressive fibrosis. Assessing DR extension at diagnosis may add valuable information related to the extent of biliary damage, to the potential to restore DCJ, and to fibrogenesis. Our result could open future perspectives on DR as a useful histologic feature for individual risk stratification and, particularly, for the identification of people who may benefit directly from a more aggressive, second-line therapy.

Abbreviations

αSMA, α-smooth muscle actin; AE2, anion exchanger 2; ALP, alkaline phosphatase; ALPt0, ALP at diagnosis; ALPt12, ALP at 12 months after UDCA therapy; ALT, alanine aminotransferase; ALTt0, ALT at diagnosis; AMA, antimitochondrial antibody; ANA, antinuclear antibody; AST, aspartate aminotransferase; ASTt0, AST at diagnosis; BAC, bile acid control; BIL, bilirubin; BILt0, BIL at diagnosis; CA, cholangitis activity; CK19, cytokeratin 19; CK7, cytokeratin 7; DCJ$^{/d}$, DCJ per ductule; DCJ$^{/pt}$, DCJ per portal tract; DCJ, ductular–canalicular junction; DR, ductular reaction; EpCAM, epithelial cell adhesion molecule; GGT, gamma-glutamyl transferase; HA, hepatitis activity; HSC, hepatic stellate cell; IH, intermediate hepatocyte; MF, myofibroblast; Muc-1, mucin 1; PBC, primary biliary cholangitis; PCNA, proliferating cell nuclear antigen; RT-qPCR, real-time quantitative PCR; SCTR, secretin receptor; SQ, semiquantitative; UDCA, ursodeoxycholic acid; ULN, upper limit of normal; URS, UDCA response score; WT, wild type.

Financial support

This study was supported by research project grants from Sapienza University of Rome (EG and PO). This work was partly supported by the Hickam Endowed Chair, Gastroenterology, Medicine, Indiana University School of Medicine; the Indiana University Health–Indiana University School of Medicine Strategic Research Initiative; the SRCS to GA and RCS to HF (1I01BX003031) from the United States Department of Veteran's Affairs; Biomedical Laboratory Research and Development Service; and NIH grants DK108959 and DK119421 (HF) and DK054811, DK115184, DK076898, and AA028711 (GA and SG). This material is the result of work supported by resources at the Richard L. Roudebush VA Medical Center, Indianapolis, IN, and Medical Physiology, Medical Research Building, Temple, TX. The views expressed in this article are those of the authors and do not necessarily represent the views of the Department of Veterans Affairs. MC, LC, AG, and PI were partially supported by the Italian Ministry of University and Research (MIUR)–Department of Excellence project PREMIA (PREcision MedIcine Approach: bringing biomarker research to clinic) and by the grants titled 'Biocompatible Nano-assemblies to Increase the Safety and the Efficacy of Steroid Treatment Against Liver Inflammation' (Grant/Award Number GR-2018-12367794).

Conflicts of interest

The authors declare that there is no conflict of interest.

Please refer to the accompanying ICMJE disclosure forms for further details.

Authors' contributions

Had access to the study data and reviewed and approved the final manuscript: All authors.
Conceptualisation: GC, VC, MC.
Methodology: DO, GC, LK, HF, PO, SG.
Investigation: VC, GC, DO, MC, LK, NZ, LC, CR, MV, DD, AG, RV.
Writing – original draft: GC, MC.
Writing – review and editing: DO, VC, AF, GA, EG, DA.
Funding acquisition: EG, DA, PO, PI.
Resources: AF, VC, MC, HF, CR, MV, DD, AG, RV.
Supervision: EG, DA, GA, PI.

Data availability statement

All data are available upon reasonable request to the authors.

Supplementary data

Supplementary data to this article can be found online at https://doi.org/10.1016/j.jhepr.2022.100556.

References

Author names in bold designate shared co-first authorship

[1] Lleo A, Wang GQ, Gershwin ME, Hirschfield GM. Primary biliary cholangitis. Lancet 2020;396:1915–1926.

[2] Hirschfield GM, Dyson JK, Alexander GJM, Chapman MH, Collier J, Hübscher S, et al. The British Society of Gastroenterology/UK-PBC primary biliary cholangitis treatment and management guidelines. Gut 2018;67:1568–1594.

[3] **D'Amato D**, **De Vincentis A**, Malinverno F, Viganò M, Alvaro D, Pompili M, et al. Real-world experience with obeticholic acid in patients with primary biliary cholangitis. JHEP Rep 2021;3:100248.

[4] Trauner M, Nevens F, Shiffman ML, Drenth JPH, Bowlus CL, Vargas V, et al. Long-term efficacy and safety of obeticholic acid for patients with primary biliary cholangitis: 3-year results of an international open-label extension study. Lancet Gastroenterol Hepatol 2019;4:445–453.

[5] **Carbone M**, **Nardi A**, Flack S, Carpino G, Varvaropoulou N, Gavrila C, et al. Pretreatment prediction of response to ursodeoxycholic acid in primary biliary cholangitis: development and validation of the UDCA Response Score. Lancet Gastroenterol Hepatol 2018;3:626–634.

[6] **Cristoferi L**, **Calvaruso V**, Overi D, Viganò M, Rigamonti C, Degasperi E, et al. Accuracy of transient elastography in assessing fibrosis at diagnosis in naive patients with primary biliary cholangitis: a dual cut-off approach. Hepatology 2021;74:1496–1508.

[7] Alvaro D, Carpino G, Craxi A, Floreani A, Moschetta A, Invernizzi P. Primary biliary cholangitis management: controversies, perspectives and daily practice implications from an expert panel. Liver Int 2020;40:2590–2601.

[8] Carbone M, Sharp SJ, Flack S, Paximadas D, Spiess K, Adgey C, et al. The UK-PBC risk scores: derivation and validation of a scoring system for long-term prediction of end-stage liver disease in primary biliary cholangitis. Hepatology 2016;63:930–950.

[9] Nakanuma Y, Zen Y, Harada K, Sasaki M, Nonomura A, Uehara T, et al. Application of a new histological staging and grading system for primary biliary cirrhosis to liver biopsy specimens: interobserver agreement. Pathol Int 2010;60:167–174.

[10] Ludwig J, Dickson ER, McDonald GS. Staging of chronic nonsuppurative destructive cholangitis (syndrome of primary biliary cirrhosis). Virchows Arch A Pathol Anat Histol 1978;379:103–112.

[11] Carpino G, Cardinale V, Folseraas T, Overi D, Floreani A, Franchitto A, et al. Hepatic stem/progenitor cell activation differs between primary sclerosing and primary biliary cholangitis. Am J Pathol 2018;188:627–639.

[12] Overi D, Carpino G, Cardinale V, Franchitto A, Safarikia S, Onori P, et al. Contribution of resident stem cells to liver and biliary tree regeneration in human diseases. Int J Mol Sci 2018;19:2917.

[13] Sato K, Marzioni M, Meng F, Francis H, Glaser S, Alpini G. Ductular reaction in liver diseases: pathological mechanisms and translational significances. Hepatology 2019;69:420–430.

[14] European Association for the Study of the Liver. EASL Clinical Practice Guidelines: management of cholestatic liver diseases. J Hepatol 2009;51:237–267.

[15] **de Vries EM**, **de Krijger M**, Färkkilä M, Arola J, Schirmacher P, Gotthardt D, et al. Validation of the prognostic value of histologic scoring systems in primary sclerosing cholangitis: an international cohort study. Hepatology 2017;65:907–919.

[16] **Roskams TA**, **Theise ND**, Balabaud C, Bhagat G, Bhathal PS, Bioulac-Sage P, et al. Nomenclature of the finer branches of the biliary tree: canals, ductules, and ductular reactions in human livers. Hepatology 2004;39:1739–1745.

[17] **Nevzorova YA**, **Boyer-Diaz Z**, Cubero FJ, Gracia-Sancho J. Animal models for liver disease – a practical approach for translational research. J Hepatol 2020;73:423–440.

[18] Williams MJ, Clouston AD, Forbes SJ. Links between hepatic fibrosis, ductular reaction, and progenitor cell expansion. Gastroenterology 2014;146:349–356.

[19] **Spee B**, **Carpino G**, Schotanus BA, Katoonizadeh A, Vander Borght S, Gaudio E, et al. Characterisation of the liver progenitor cell niche in liver diseases: potential involvement of Wnt and Notch signalling. Gut 2010;59:247–257.

[20] Lindor KD, Bowlus CL, Boyer J, Levy C, Mayo M. Primary biliary cholangitis: 2018 practice guidance from the American Association for the Study of Liver Diseases. Hepatology 2019;69:394–419.

[21] European Association for the Study of the Liver. EASL Clinical Practice Guidelines: the diagnosis and management of patients with primary biliary cholangitis. J Hepatol 2017;67:145–172.

[22] Angulo P, Larson DR, Therneau TM, LaRusso NF, Batts KP, Lindor KD. Time course of histological progression in primary sclerosing cholangitis. Am J Gastroenterol 1999;94:3310–3313.

[23] Burak KW, Angulo P, Lindor KD. Is there a role for liver biopsy in primary sclerosing cholangitis? Am J Gastroenterol 2003;98:1155–1158.

[24] Warnes T, Roberts S, Smith A, Haboubi N, McMahon RF. Liver biopsy in primary biliary cholangitis: is sinusoidal fibrosis the missing key? J Clin Pathol 2019;72:669–676.

[25] Murillo Perez CF, Hirschfield GM, Corpechot C, Floreani A, Mayo MJ, van der Meer A, et al. Fibrosis stage is an independent predictor of outcome in primary biliary cholangitis despite biochemical treatment response. Aliment Pharmacol Ther 2019;50:1127–1136.

[26] **Gadd VL**, **Aleksieva N**, Forbes SJ. Epithelial plasticity during liver injury and regeneration. Cell Stem Cell 2020;27:557–573.

[27] Govaere O, Cockell S, Van Haele M, Wouters J, Van Delm W, Van den Eynde K, et al. High-throughput sequencing identifies aetiology-dependent differences in ductular reaction in human chronic liver disease. J Pathol 2019;248:66–76.

[28] Smit JJ, Schinkel AH, Oude Elferink RP, Groen AK, Wagenaar E, van Deemter L, et al. Homozygous disruption of the murine mdr2 P-glycoprotein gene leads to a complete absence of phospholipid from bile and to liver disease. Cell 1993;75:451–462.

[29] **Cariello M**, **Piccinin E**, Garcia-Irigoyen O, Sabbà C, Moschetta A. Nuclear receptor FXR, bile acids and liver damage: introducing the progressive familial intrahepatic cholestasis with FXR mutations. Biochim Biophys Acta Mol Basis Dis 2018;1864:1308–1318.